DOI: 10.1002/adma.200700448

A Combined Top-Down/Bottom-Up Approach for the Nanoscale Patterning of Spin-Crossover Coordination Polymers**

By *Gábor Molnár*,* *Saioa Cobo*, *José Antonio Real*, *Franck Carcenac*, *Emmanuelle Daran*, *Christophe Vieu*, and *Azzedine Bousseksou**

Molecular spin-crossover complexes of $3d^4$–$3d^7$ transition-metal ions have been the focus of many researchers' work because of their fascinating properties associated with the bistability of their electronic states (high spin (HS) or low spin (LS)).[1] Although the origin of the spin-crossover phenomenon is purely molecular, the macroscopic behavior of these systems in the solid state is strongly determined by the interactions, of mainly elastic origin, between the transition-metal ions.[2]

Recently, remarkable progress has been made in the area of spin-crossover complexes with infinite one-, two-, or three-dimensional (1D, 2D, 3D) networks, the so-called coordination polymers.[3] The purpose of this approach was the enhancement and fine tuning of cooperative properties by the strong covalent links between the metallic centers in the polymers.[4] Indeed, a number of highly cooperative polymer systems have been reported in the recent literature that display hysteretic behavior (thermal and piezo), in some cases even at room temperature. In addition to this, we have recently demonstrated that 3D coordination polymers represent an attractive platform for growth of surface thin films with spin-crossover properties.[5] In fact, the 3D network structure allows the sequential assembly, via stepwise adsorption reactions, of multilayer films based entirely on intra- and interlayer coordination bonds. These films have opened up possibilities for investigating size-reduction effects, optical and dielectric properties, and device applications of spin-crossover materials.[6]

A further step in this direction is the generation of micro- and nanometer-sized lateral patterns. In fact, the multilayer sequential assembly (MSA) process (also called directed assembly or layer-by-layer assembly in the literature[7]) has become increasingly popular not only for fabricating thin films but also many efforts have been devoted to generating distinct patterns of the multilayer films. Various lithographic and non-lithographic methods—such as deposition on chemically patterned surfaces, inkjet printing, lift-off processes, etching, direct photopatterning, and microcontact printing—have been explored with this aim.[8] Each method has, of course, different merits, but the lift-off process remains an industry standard owing to its simplicity and reliability. Furthermore, when combined with electron-beam lithography (EBL), it allows patterns to be obtained in a wide size range down to the sub-10 nm limit,[9] and the alignment of the patterns is also possible with respect to structures that may already exist on the substrate.

In this Communication, we report on a process for nano- and microscale assembly of the 3D spin-crossover coordination polymer Fe(pyrazine)[Pt(CN)$_4$] (**1**) (Scheme 1) by using a combination of top-down (lift-off) and bottom-up (MSA) methods. We call attention to the 3D polymer nature of this system, which is the key aspect for 1) obtaining room-temperature hysteresis, 2) assembling multilayers, and 3) performing

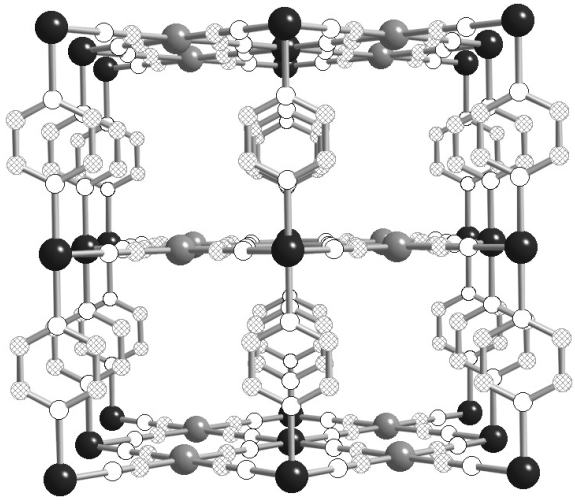

Scheme 1. The 3D coordination network of Fe(pyrazine)[Pt(CN)$_4$] (Atom code: Fe(II), black; Pt(II), grey; C, hollow hatched; N, white).

[*] Dr. G. Molnár, Dr. A. Bousseksou, S. Cobo
Laboratoire de Chimie de Coordination
Centre National de la Recherche Scientifique
UPR8241, 205 route de Narbonne, 31077 Toulouse (France)
E-mail: molnar@lcc-toulouse.fr; boussek@lcc-toulouse.fr
Prof. J. A. Real
Instituto de Ciencia Molcular
Universidad de Valencia, Edificio de Institutos de Paterna
P.O. Box 22085, 46071 Valencia (Spain)
F. Carcenac, Dr. E. Daran, Prof. C. Vieu
Laboratoire d'Analyse et d'Architecture des Systèmes
Centre National de la Recherche Scientifique
UPR8001, 7 avenue du Colonel Roche, 31077 Toulouse (France)

[**] This work was supported by the RTB program of the LAAS-CNRS. The authors are grateful for financial support from the Agence National de la Recherche (project NANOMOL), from the Spanish Ministerio de Educación y Ciencia (CTQ 2004-03456/BQU) and from the European Action COST D35.

ADVANCED MATERIALS

lift-off. In fact, lift-off becomes possible because of the extreme insolubility of the coordination network when compared to that of the molecular spin-crossover complexes.

Compound **1** is made up of (pseudo-)octahedral iron(II) cations and square-planar $[Pt(CN)_4]^{2-}$ anions. Each CN group coordinates an iron(II) atom. Four CN groups saturate its equatorial positions, defining $\{Fe[Pt(CN)_4]\}_n$ layers, while the remaining axial positions are occupied by two pyrazine molecules, which act as bridges connecting the iron atoms of two adjacent $\{Fe[Pt(CN)_4]\}_n$ layers. This compound displays a strongly cooperative spin transition with a ca. 25 K wide hysteresis loop centered around room temperature both in powder[10] and thin film[5] forms. Furthermore, it exhibits a pressure-[11] and light-induced[12] spin-state switching at room temperature. These results, together with the fact that the porous structure may adsorb and desorb small guest molecules,[13] are all relevant for applications.

The process to obtain patterns of **1** is presented schematically in Scheme 2. A gold-coated silicon surface was covered by a conventional polymethylmethacrylate (PMMA) EBL resist, in which square-shaped patterns of different size and density have been written by a focused electron beam. After resist development, the substrates were dipped into a solution of 4,4′-azopyridine to prepare an anchoring layer for the thin film. According to literature data,[14] 4,4′-azopyridine forms a fairly continuous monolayer and adopts a perpendicular orientation on silver surfaces with respect to the plane of the molecule (Scheme 3). We suppose that in the case of our gold substrates a similar orientation might occur since we found that this layer facilitates the build up of films of compound **1**. These latter were assembled in the next step via the successive adsorption of Fe^{2+}, $[Pt(CN)_4]^{2-}$ and pyrazine from dilute solutions (15 cycles). Since we used ethanol solvent, dissolution of the PMMA structures is not expected during the film deposition. Multilayer deposition took place both in the openings of the resist as well as on top of the PMMA. Finally, the patterns were transferred by lifting off the PMMA. The good adherence of the insoluble film of **1** on the surface allowed us using ultrasonic assistance in order to completely remove the resist.

As shown in the scanning electron microscopy (SEM) images of Figure 1, clear patterns of various size (between 2 μm and 50 nm) were created. These patterns exhibit square shapes with sharp borders for feature sizes between 2 μm and 200 nm. (Larger patterns, not shown here, gave similar results.) We could also successfully lift dense arrays of sub-micrometer features with periods down to 200 nm. Patterns with smaller periods turned out to be unsuitable for lift-off. This limit can certainly be improved somewhat by decreasing the number of deposition cycles (i.e., the film thickness). It should also be noted that arrays can be produced with features below 200 nm, but many defects are present (almost independently of the array density) in this size range. A typical example is shown in Figure 1f. Figure 1 also shows some patterns obtained by evaporation of gold on the PMMA patterns and lift-off. We use this metal for comparison as it is expected to give high-quality patterns on our substrates. We can see that the shape of the patterns of **1** compares well to the gold patterns at 200 nm, but at smaller sizes the latter pattern gives significantly better results in terms of reproducibility. This finding is related to the fact that **1** is deposited from the liquid phase, and when the openings in the resist are relatively small, wetting of the substrate becomes increasingly difficult. Moreover, the kinetics of the deposition must also be altered in such confined reaction volumes. In general, we also found that patterns of **1** could be obtained using relatively small exposure doses when compared to gold. For example, from the former, we could produce arrays of 200 nm squares with a 400 nm period for a dose of 165 $\mu C\,cm^{-2}$, while doses higher than 210 $\mu C\,cm^{-2}$ were necessary to fabricate the same pattern from Au. The most probable explanation for this observation is that ethanol is not completely innocent in this process and acts as a very slow developer on PMMA.

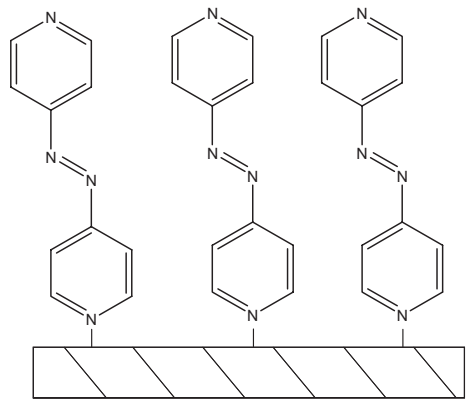

Scheme 3. Depiction of the 4,4′-azopyridine anchoring layer.

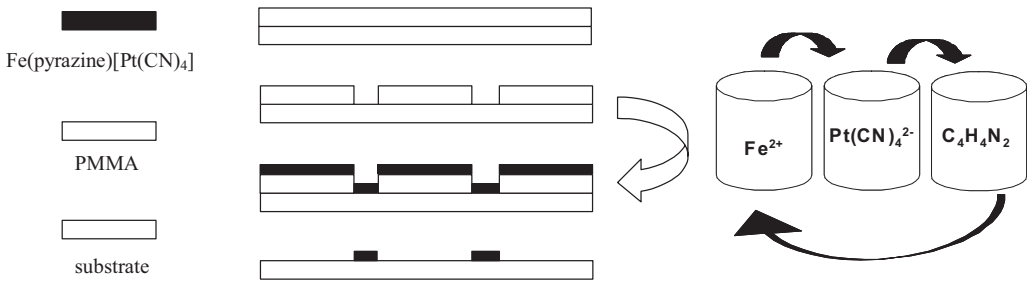

Scheme 2. Schematic procedure for the patterning of compound **1**.

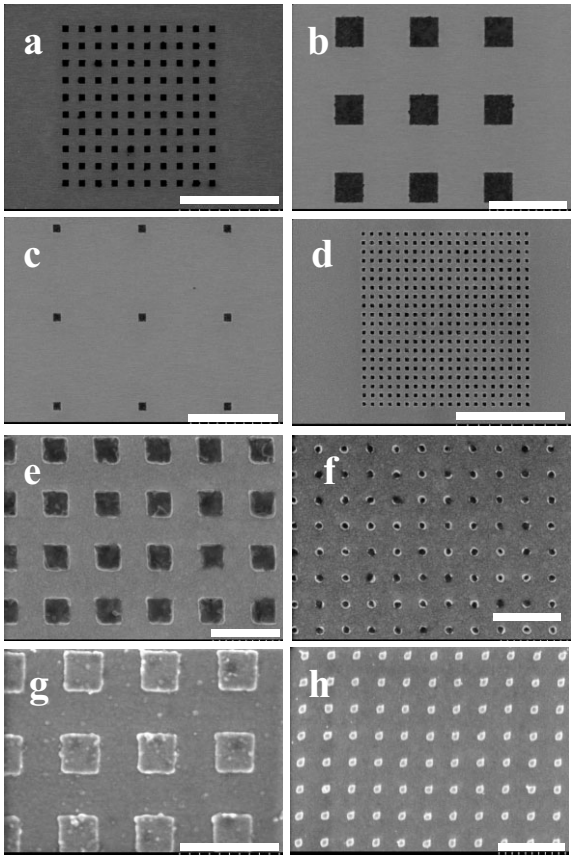

Figure 1. SEM images of patterns of **1** after 15 deposition cycles with pattern size of a,b) 2 μm, c) 500 nm, d,e) 200 nm, f) 50 nm, and gold patterns of g) 200 nm and h) 50 nm size. The scale bars are 30 μm (a), 5 μm (b–d), and 500 nm (e–h).

Atomic force microscopy (AFM) studies of these patterns gave rather surprising results. We found that as the lateral size of the patterns decreases, their height decreases as well. For 15 deposition cycles the mean height of 2 μm, 200 nm, and 50 nm large squares is ca. 150 nm, 40 nm, and 12 nm, respectively. For lateral sizes above 0.5 μm, the pattern heights remain fairly constant (Fig. 2). In fact, the wetting of the surface becomes more difficult as the openings in the resist get smaller. We believe that this effect, coupled with mass-transport limitations of the MSA components in the small reaction volumes, leads to decreased deposition rates for small patterns.[15] These effects can probably be limited by optimizing the anchoring layer, solvent, dipping time, and temperature for each application, but this work is out of the scope of the present Communication.

It is important to note that the film thickness on large surfaces considerably exceeds what could be expected for the formation of a single "layer" in three sequential adsorption steps (i.e., one cycle) since the thickness of a layer is only ca. 1 nm. This finding seems rational for us, taking into account a 3D-growth scheme from a number of surface nucleation sites, but it is in significant disagreement with the report of Mallouk and co-workers on the growth of Ni(4,4′-bipyridine)[$Pt(CN)_4$]

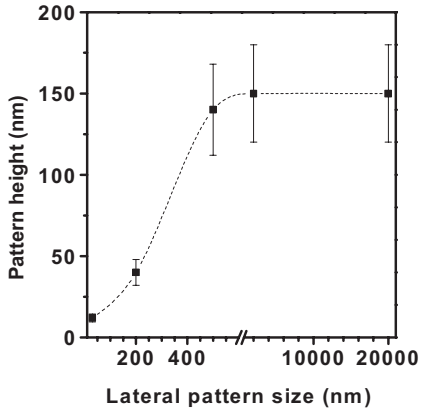

Figure 2. Evolution of pattern heights of **1** as a function of the lateral pattern size, following 15 deposition cycles. (The dashed line is inserted to guide the eye.)

coordination polymers.[16] One should also be aware that in contrast to the idealized layer-by-layer deposition scheme of polyionic organic compounds,[7] the assembly of **1** involves not only adsorption steps but also desorption and re-adsorption accompanied by the formation of crystallites. As suggested in the literature,[17] we have tried to minimize such phenomena by keeping the dipping times as short as possible. However, the observation of surface details clearly reveals that the films are composed of 3D crystallites with substantial roughness at large thickness (Fig. 3).

To control the composition and structure of these micro- and nanometer-sized objects as well as to probe the spin state, we carried out Raman spectroscopy measurements. In the past, we successfully employed this technique to investigate thin films of **1**.[5] The Raman spectra of this compound exhibit intense pyrazine internal vibrational modes between 600 and 1600 cm^{-1}. To probe the spin-state change, several modes may be followed, but the strong intensity enhancement of the Raman mode at 1230 cm^{-1} when going from the HS to the LS state is probably the most useful marker. When normalized to the intensity of the 1030 cm^{-1} peak, this mode provides a

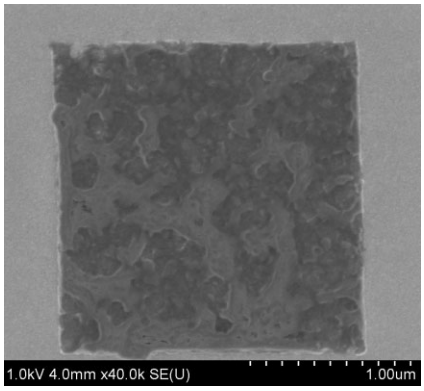

Figure 3. Low-energy SEM image of a 2 μm pattern (ca. 150 nm thick) of **1**, showing the surface details.

ADVANCED MATERIALS

quantitative measurement of the spin state.[5] Figure 4 shows selected Raman spectra of patterned films of **1** recorded at 295 and 80 K, for different pattern sizes following 15 deposition cycles. Spectra were recorded following an annealing process at 150 °C, which was necessary to remove solvent residue (ethanol, trichloroethylene, water) and to obtain reproducible spectra. Spectra obtained from patterns with sizes ≥2 μm were found to be very similar, which is not surprising if one takes into account the laser spot diameter (ca. 3 μm). In this size range, the HS-to-LS spin-state change is easily detected via the strong intensity enhancement of the 1230 cm^{-1} Raman mode (Fig. 4a), and, quite predictably, the spin-crossover properties were found to be the same as those obtained previously on continuous thin films.[5] At smaller pattern sizes, the quantity of the matter probed by the laser beam decreases significantly, and to record convenient spectra the excitation power and time must be increased considerably. This leads, in turn, to laser heating of the sample to some extent and the pure LS spectrum is thus difficult to obtain. We could, however, record spectra (Fig. 4b and c) of a single 500 nm object (Fig. 1c) and an array of 200 nm patterns (Fig. 1e), respectively, exhibiting spin-state change. To our knowledge, these are the smallest objects for which a spin-crossover phenomenon has been observed up to now. Since conventional Raman microscopy is not suitable for the investigation of smaller patterns, other methods are currently under development for this purpose.

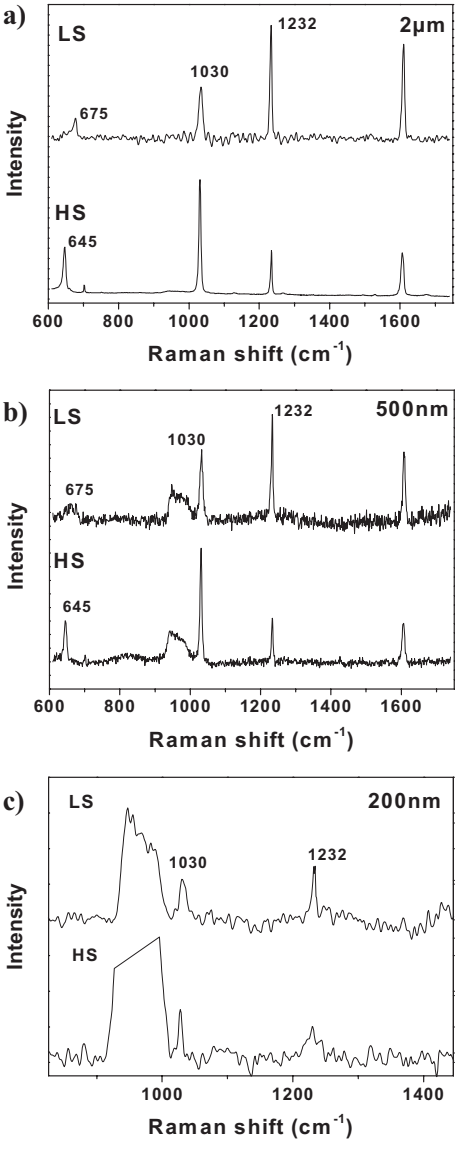

Figure 4. Raman spectra (excited at 632.8 nm) of patterned thin films of **1** in the HS (295 K) and LS (80 K) states. Spectra were acquired from: a) a single 2 μm pattern, b) a single 500 nm pattern, and c) approximately 45 patterns (array) of 200 nm size.

In conclusion, we have demonstrated that micro- and nanometer-sized patterns of the spin-crossover coordination polymer Fe(pyrazine)[$Pt(CN)_4$] (**1**) can be obtained using a PMMA mask as a physical barrier for the assembly of the multilayer film on the gold surface. The key issue here is achieving a high spatial resolution while retaining spin-crossover properties. These properties are tunable as the process allows replacing (either partly or completely) of the different "bricks" of the network. Differences in the film thickness as a function of the lateral pattern size have been observed in the sub-micrometer range, which can be explained by differences in wetting as well as in the reaction kinetics within the small reaction volumes. Further studies are thus necessary to optimize the deposition conditions. The fabrication and the initial physical characterization of the micro- and nanometer patterns of **1** support the utility of this technique for use in studies aimed at elucidating important size–property relationships, but the usefulness of the fabrication method is much broader and may also impact applications of spin-crossover materials in optical[18] and electronic[6] devices. Work in these directions is in progress.

Experimental

Nanofabrication: Initially, the polished 4 in. silicon wafer (p-type, 10 $\Omega\,cm^{-1}$) was covered by 5 nm of titanium and 15 nm of gold, deposited by thermal evaporation at a pressure of 5×10^{-7} mbar (1 mbar = 100 Pa) using a Veeco 770 thermal evaporator apparatus. After it was cleaned in a saturated mixture of chromium trioxide in sulfuric acid (95 %), a PMMA (weight-average molecular weight: 950 000, 30 $g\,L^{-1}$ in methyl isobutyl ketone, MIBK) EBL resist layer of ca. 150 nm thickness was spun on the gold surface at a speed of 3000 rpm for 30 s. The resist was cured at 175 °C for 2 min and patterned by using a Raith150 electron-beam writer operated at 20 kV with a beam current of 116 pA and a spot size of 10 nm. Each pattern was written several times using different irradiation doses, ranging from 150 to 300 $\mu C\,cm^{-2}$. Subsequently, the wafer was cut into 7 mm × 7 mm pieces (each containing the same pattern) for various experiments. The exposed resist was developed in a 1:3 mixture of MIBK/IPA (isopropyl alcohol) solution at 20 °C for 45 s. The sample was soaked in pure IPA for 30 s to stop the developing process and dried in a nitrogen flow. After development, thin films of **1** were deposited on the substrate as follows. The substrates were first functionalized by submerging them overnight in a solution of 30 mM 4,4′-azopyridine (synthesized according to [19]) in ethanol at room

temperature. These wafers were first cleaned in pure ethanol and then soaked alternately (total of 15 cycles) in ethanol solutions of 50 mM $Fe(BF_4)_2 \cdot 6H_2O$, 50 mM (tetrabutylammonium)$_2Pt(CN)_4$, and 50 mM pyrazine (1 min) at –60 °C under a nitrogen atmosphere, with rinsing in pure ethanol between steps (30 s). Finally, the wafers were dried under a nitrogen flow. Alternatively, on some substrates a 20 nm gold film was evaporated after development at a pressure of 5×10^{-7} mbar with a rate of 20 Å s^{-1}. Finally, lift-off was achieved by immersing the wafer in hot (ca. 60 °C) trichloroethylene for 2 min followed by 5 min agitation in an ultrasonic bath (at room temperature).

Characterization: AFM investigations were performed with a Nanoscope III (Veeco, Digital Instruments) microscope equipped with a Si tip (Nano-world Arrow NC). Scans were performed in air at room temperature at 1 Hz rate in the tapping mode. SEM images were recorded with a Hitachi S-4800 microscope operating at 1 keV. Variable-temperature Raman spectra were collected in the 150–2300 cm^{-1} frequency range either in ambient conditions or under nitrogen on the cold finger of a THMS600 (Linkam) liquid nitrogen cryostage. Before the measurements, the samples were heated in a nitrogen flow to 150 °C for 30 min to eliminate residues of solvents. The LabRAM-HR (Jobin Yvon) Raman spectrometer used in these experiments consists of a BXFM (Olympus) optical microscope, a single-grating spectrograph (600 grooves mm^{-1}, focal length, $f = 800$ mm) and a DU420-OE (Andor) charge-coupled device (CCD) detector. The entrance slit was kept at 100 µm and a spectral resolution of ca. 4 cm^{-1} was obtained. The 632.8 nm line of a 17 mW He–Ne laser was used as the excitation source, and plasma lines were removed using a narrow-band interference filter. The exciting radiation was directed through appropriate neutral density filters ($2 \geq$ optical density ≥ 0) and was focused on the sample via a ×50, long-working-distance objective (numerical aperture, NA = 0.5). The scattered light was collected in a backscattering configuration, using the same microscope objective, and the Rayleigh scattering was removed by means of a holographic notch filter.

Received: February 21, 2007
Revised: May 4, 2007
Published online: July 17, 2007

[1] a) *Spin Crossover in Transition Metal Compounds I–III*, Topics in Current Chemistry (Eds: P. Gütlich, H. A. Goodwin), Vol. 233–235, **2004**. b) P. Gütlich, A. Hauser, H. Spiering, *Angew. Chem. Int. Ed. Engl.* **1994**, *33*, 2024. c) A. Bousseksou, G. Molnár, G. Matouzenko, *Eur. J. Inorg. Chem.* **2004**, 4353. d) J. A. Real, A. B. Gaspar, M. Carmen Munoz, *J. Chem. Soc., Dalton Trans.* **2005**, 2062.

[2] H. Spiering, K. Boukheddaden, J. Linarès, F. Varret, *Phys. Rev. B* **2004**, *70*, 184 106.

[3] a) J. Kröber, E. Kodjovi, O. Kahn, F. Grolière, C. Jay, *J. Am. Chem. Soc.* **1993**, *115*, 9810. b) Y. Garcia, V. Niel, M. Carmen Munoz, J. A. Real, *Top. Curr. Chem.* **2004**, *233*, 229. c) J. A. Real, A. B. Gaspar, V. Niel, M. C. Munoz, *Coord. Chem. Rev.* **2003**, *236*, 121.

[4] O. Kahn, C. Jay-Martinez, *Science* **1998**, *279*, 44.

[5] S. Cobo, G. Molnár, J. A. Real, A. Bousseksou, *Angew. Chem. Int. Ed.* **2006**, *45*, 5786.

[6] a) A. Bousseksou, C. Vieu, J.-F. Létard, P. Demont, J.-P. Tuchagues, L. Malaquin, J. Menegotto, L. Salmon, *EP 1430552*, **2004**. b) A. Bousseksou, G. Molnár, S. Cobo, L. Salmon, J. A. Real, C. Vieu, *PCT/FR2007/000297*.

[7] a) G. Decher, *Science* **1997**, *277*, 1232. b) *Multilayer Thin Films* (Eds: G. Decher, J. B. Schlenoff), Wiley-VCH, Weinheim, **2003**.

[8] P. T. Hammond, *Adv. Mater.* **2004**, *16*, 1271.

[9] C. Vieu, F. Carcenac, A. Pépin, Y. Chen, M. Mejias, A. Lebib, L. Manin-Ferlazzo, L. Couraud, H. Launois, *Appl. Surf. Sci.* **2000**, *164*, 111.

[10] V. Niel, J. M. Martínez-Agudo, M. C. Muñoz, A. B. Gaspar, J. A. Real, *Inorg. Chem.* **2001**, *40*, 3838.

[11] G. Molnár, V. Niel, J. A. Real, L. Dubrovinsky, A. Bousseksou, J. J. McGarvey, *J. Phys. Chem. B* **2003**, *107*, 3149.

[12] S. Bonhommeau, G. Molnár, A. Galet, A. Zwick, J. A. Real, J. J. McGarvey, A. Bousseksou, *Angew. Chem. Int. Ed.* **2005**, *44*, 4069.

[13] S. Kitagawa, R. Kitaura, S. Noro, *Angew. Chem. Int. Ed.* **2004**, *43*, 2334.

[14] Z. Zhuang, J. Cheng, X. Wang, Y. Yin, G. Chen, B. Zhao, H. Zhang, G. Zhang, *J. Mol. Struct.* **2006**, *794,* 77.

[15] O. Crespo-Biel, B. Dordi, P. Maury, M. Peter, D. N. Reinhoudt, J. Huskens, *Chem. Mater.* **2006**, *18,* 2545.

[16] C. M. Bell, M. F. Arendt, L. Gomez, R. H. Schmell, T. E. Mallouk, *J. Am. Chem. Soc.* **1994**, *116*, 8374.

[17] W. Jin, A. Toutianoush, M. Pyrasch, J. Schnepf, H. Gottschalk, W. Rammensee, B. Tieke, *J. Phys. Chem. B* **2003**, *107,* 12 062.

[18] P. Mounaix, E. Freysz, J. Degert, N. Daro, J.-F. Létard, P. Kuzel, V. Vigneras, L. Oyenhart, *Appl. Phys. Lett.* **2006**, *89*, 174 105.

[19] J.-P. Launay, M. Tourrel-Pagis, J.-F. Lipskier, V. Marvaud, C. Joachim, *Inorg. Chem.* **1991**, *30*, 1033.

